Organic Matter Stoichiometry, Flux, and Oxygen Control Nitrogen Loss in the Ocean

Andrew R. Babbin,[1]* Richard G. Keil,[2] Allan H. Devol,[2] Bess B. Ward[1]

Biologically available nitrogen limits photosynthesis in much of the world ocean. Organic matter (OM) stoichiometry had been thought to control the balance between the two major nitrogen removal pathways—denitrification and anammox—but the expected proportion of 30% anammox derived from mean oceanic OM is rarely observed in the environment. With incubations designed to directly test the effects of stoichiometry, however, we showed that the ratio of anammox to denitrification depends on the stoichiometry of OM supply, as predicted. Furthermore, observed rates of nitrogen loss increase with the magnitude of OM supply. The variable ratios between denitrification and anammox previously observed in the ocean are thus attributable to localized variations in OM quality and quantity and do not necessitate a revision to the global nitrogen cycle.

The processes that remove nitrogen (N) from the ocean are (i) anaerobic ammonium oxidation (anammox), the autotrophic oxidation of ammonium to N_2 by nitrite, and (ii) denitrification, a stepwise heterotrophic reduction of nitrate (the most abundant species of fixed N in the ocean) to N_2. The existence of anammox was contemplated even before the anammox metabolism was discovered in bacteria (*1*, *2*), based on the observation that ammonium, a by-product from the heterotrophic respiration of N-containing organic matter (OM), does not accumulate within strictly anoxic environments (*3*), such as the oxygen-deficient zones (ODZs). Because ammonium cannot be removed by oxidation via conventional aerobic nitrification in ODZs, the oxidation of the particulate organic matter (POM)–derived ammonium must occur through anammox. Building on previous work (*4*), we derived a balance between anammox and denitrification from generic OM stoichiometry rather than from average ocean POM by assuming (i) complete oxidation of POM to CO_2, (ii) no accumulation of ammonium or nitrite, and (iii) that all ammonium liberated by the reduction of nitrate and nitrite must be oxidized via anammox in the absence of molecular O_2. The equation stoichiometry is predicated on previous theoretical (*4*) and experimental (*5*) studies that determined the species coefficients, depending on the elemental composition of the POM (see the supplementary materials). From this theoretical balance, the fraction of total N loss via anammox is

$$f_{amx} = \frac{1.02\frac{N}{C}}{0.4 + 0.1\frac{H}{C} - 0.2\frac{O}{C} + 0.456\frac{N}{C}} \quad (1)$$

where the variables are the ratios of each of the major elements in the POM substrate with respect to C. From Eq. 1, it becomes apparent that the C/N ratio is the most important parameter in setting the balance, because (i) the N content is modified by the largest coefficient, and (ii) the H and O contents tend to compensate for each other. For the average labile POM stoichiometry in the ocean, $C_{6.6}H_{10.9}O_{2.6}N$ (*6*), $f_{amx} = 28\%$.

It is somewhat mysterious then that anammox and denitrification often do not appear to be stoichiometrically linked, given the generally conserved average composition (C/N = 6.6) of OM, but rather that one process or the other dominates the total N loss when measured discretely in space and time (*7*, *8*). Spatiotemporal dynamics (*7*) and failure to include the effect of episodic POM supply in small-volume incubations are likely explanations, although so far unproven. Others have invoked alternative anaerobic mechanisms, such as dissimilatory nitrate reduction to ammonium (*8*), or benthic ammonium release (*9*), to provide ammonium for anammox in the absence of measurable denitrification, but these explanations cannot fully satisfy the anammox demand for ammonium. Recently, an extensive data set from the South Pacific showed that on a larger (areal) scale, anammox was 28% of the total N loss (*10*), as predicted (*4*) by the average composition of the OM (i.e., C/N = 6.6). However, most sites had low rates of anammox and even lower rates of denitrification, whereas a few discrete locations had very high denitrification rates. The balance between anammox and denitrification is important for understanding N cycling and the energy balance in suboxic zones, and because the two processes have different effects on C mineralization and on the production and consumption pathways of nitrous oxide, a major greenhouse gas and ozone-depleting agent (*11*), which is a significant intermediate in the denitrification pathway but not of anammox (*12*).

To investigate the roles of OM stoichiometry and O_2 concentration in controlling N loss in the Eastern Tropical North Pacific ODZ, we performed incubation experiments using isotopically labeled nitrite as a tracer and various OM treatments at the top of the ODZ and the secondary nitrite maximum of two stations, one coastal and one offshore (fig. S1). Anammox and denitrification rates increased by different proportions in response to specific OM additions, with higher proportions of anammox corresponding to greater N relative to C content (i.e., a lower C/N ratio) of the source substrate (Table 1). Experimental treatments included sterilized substrate organic compositions of $C_{9.7}H_{17.8}O_{8.9}NH_3$ for the sucrose and ammonium mixture, $C_{3.6}H_{5.7}ON$ for the casamino acids, and $C_{6.8}H_{11.2}O_{2.7}N$ for the sinking particulate OM (from the average measured POM C/N, with an inferred C/H/O from average POM stoichiometry) (*6*). Based on experiments at both depths of each of the two stations (Fig. 1), the predicted anammox proportions of N loss of 22, 45, and 27% (Eq. 1), respectively, match the observed values quite closely (Fig. 2). These data confirm that the proportions of the two N loss processes depend on the stoichiometry of the source OM.

The addition of fresh OM-induced changes in observed anammox and denitrification rates, indicating that the total fixed N loss must have been prevailingly limited by OM supply, probably because any ambient dissolved OM before the addition was highly refractory (*13*). This is confirmed by the measured increase of N loss rates from the addition of OM, regardless of stoichiometry, in 11 of 12 experiments; relative to no OM addition, these rates were stimulated by factors averaging 1.4, 2.4, and 7.0 (Fig. 1) by the addition of sucrose plus ammonium, casamino acids, and sinking POM, respectively. Furthermore, the same anammox rates were observed in the sucrose additions, compared with the no OM–added treatments at the same depths, so ambient OM contributed no ammonium during the incubations. The collected sinking POM induced a much greater increase in the rates as compared with the sucrose and casamino acids treatments, despite there being a lower amount of organic C amended. This indicates that a mixture of diverse organic compound classes in naturally occurring OM is more beneficial to cell growth, perhaps by lowering the energy requirements to build and maintain cells, as compared with a pure carbohydrate or amino acid diet.

The depth distribution of total N loss rates at both stations (Fig. 3), determined from separate experiments with only labeled nitrite tracer added, further supports the link between in situ rates and OM flux. The measured rates decreased as a function of depth, in accordance with a simple power scaling law (*14*) with an exponent of –1.3. The total areal flux (obtained by integrating the rates with respect to depth) must thus vary as a function of depth with an exponent one unit higher, or –0.3. The value of –0.3 matches that of the sinking POM flux commonly measured in suboxic basins (compared with a global average of –0.8) (*14*–*18*). This remarkable correspondence indicates that denitrification is responsible for the organic C remineralization, which in turn drives N loss in the anoxic depths of the water column.

Dissolved O_2 concentrations themselves constrain the domain within the global ocean where N loss can occur, due to the preferential use of O_2 over nitrate as a terminal electron acceptor

[1]Department of Geosciences, Princeton University, Guyot Hall, Princeton, NJ 08544, USA. [2]School of Oceanography, University of Washington, Box 357940, Seattle, WA 98195, USA.

*Corresponding author. E-mail: babbin@princeton.edu

in the remineralization of OM and the regulation by O_2 of the enzymes catalyzing N loss (*19*). Marine zones where denitrification and anammox can occur have been defined variously as waters with an upper O_2 concentration of 2 to 20 μmol liter^{-1} (*20*–*23*). Although this uncertainty in threshold may seem trivial, when integrated over the volume of the ocean, the total volumes of subthreshold water decrease greatly as O_2 concentrations approach zero (*24*), and therefore the actual threshold for anaerobic processes has important implications for modeling the global N budget.

The effect of O_2 on N loss rates was distinct and apparently immediate: The addition of 3 or 8 μmol liter^{-1} of O_2 with 3 μmol liter^{-1} of NH_4^+ resulted in insignificant N loss rates, suggesting that the O_2 tolerance limit for environmental assemblages is similar to that inferred from cultured organisms (*25*). Low levels of anammox consistently occurred in the 3 μmol liter^{-1} of O_2 treatment but not at 8 μmol liter^{-1}, whereas denitrification was not consistently detected with either 3 or 8 μmol liter^{-1} of O_2. This O_2 tolerance is consistent with results from (i) the Baltic Sea (*26*), where an O_2 level of 3 μmol liter^{-1} inhibited anammox and denitrification by 90 and 100%, respectively; (ii) the Black Sea (*21*), where the anammox O_2 tolerance was estimated to be between 8 and 13 μmol liter^{-1}; and (iii) the Eastern Tropical South Pacific (*23*), where samples from the core of the ODZ exhibited no anammox when amended with O_2 greater than 3.5 μmol liter^{-1}. The slight variation in the two O_2 tolerances may allow anammox to be coupled to aerobic nitrification in water with low but nonzero O_2. But the magnitude of this difference and the steepness of the observed O_2 gradient overlying the ODZ (4 μmol liter^{-1} of O_2 m^{-1}) are such that the amount of anammox supported independently from denitrification in the ODZs must be negligible.

Rates of anammox and denitrification can be calculated based on the stoichiometry and rates of the OM flux, the exponent of the power law, and the depths bounding the anoxic zone. On the basis of this simple model, the particle fluxes of 24 and 10 mg of C m^{-2} day^{-1} measured in this study (Table S2) at the top of the coastal and offshore ODZs, respectively, should support local N_2 production rates at the top of the ODZ of 17 and 4 nmol of N liter^{-1} day^{-1}. These rates derived from the measured POM flux are comparable to those measured in the small-vial incubations of 22 and 4 nmol of N liter^{-1} day^{-1} near the depths of sediment trap deployment, and are well within errors associated by bridging two highly disparate types of measurements. The direct agreement between the calculated and measured rates provides evidence that N gas production is causally related to the organic C sedimentation flux and confirms that this simple model may be useful to estimate N loss rates in ODZs. Furthermore, using C flux data from the Mexican margin (*27*), we can predict the associated N gas production that occurs by differentiating with depth the organic flux driving this oxidation (Fig. 3A). The N_2 production rates implied by these organic C data correspond closely to our measured rates, with rates highest near the surface and decreasing via a power law scaling with depth (Fig. 3B).

In addition to providing an explanation for the relative rates of anammox and denitrification

Table 1. Anammox percent for each OM treatment. Anammox percentages are included for both sampling sites at the base of the oxycline and at the depth of the secondary nitrite maximum (SNM).

Treatment	OM stoichiometry	N/C	C oxidation state	Site				Average ± standard error
				Coastal		Offshore		
				Oxycline 60 m	SNM 100 m	Oxycline 100 m	SNM 150 m	
NH_4^+ only	—	—	—	39.8%	55.8%	33.5%	42.5%	42.9 ± 4.5%
Sucrose + NH_4^+	$C_{9.7}H_{17.8}O_{8.9}NH_3$	0.10	0	25.3%	24.5%	26.5%	21.8%	24.5 ± 1.0%
Sinking POM	$C_{6.8}H_{11.2}O_{2.7}N$	0.15	–0.41	31.2%	29.7%	32.8%	28.3%	30.5 ± 1.0%
Casamino acids	$C_{3.6}H_{5.7}ON$	0.28	–0.19	44.1%	48.3%	40.7%	41.7%	43.7 ± 1.8%

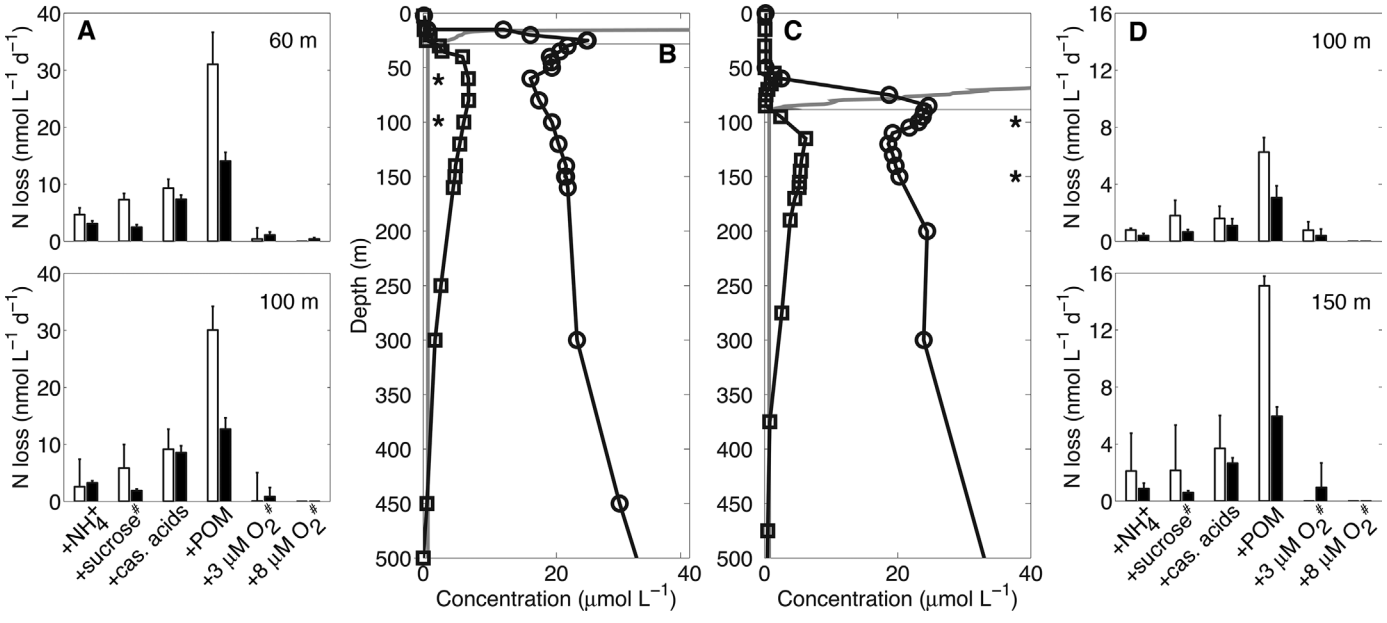

Fig. 1. Measured N loss rates. Biogeochemical parameters (center panels) measured at coastal (**A** and **B**) and offshore (**C** and **D**) sites. Nitrate (circles), nitrite (squares), and O_2 (dark-gray line) concentrations are shown. The horizontal light-gray line indicates the depth of the onset of anoxia. Asterisks indicate depths where experiments were performed, and hash marks in (A) and (D) indicate additions supplemented by $^{14}NH_4^+$. Denitrification (open bars) and anammox (solid bars) rates are shown. Error bars indicate the standard deviation of rates derived from a linear fit to five time points measured in triplicate.

in ODZs and a quantitative relationship between N loss and the flux of OM, the results presented here also have the potential to explain much of the variability in the relative contributions of anammox and denitrification rates observed in the ODZs. Although the average OM C/N in the ocean is 6.6, large variations are observed, based on the phytoplankton community composition or the state of remineralization of the OM (*14*, *28*). For instance, newly formed OM rich in amino acids can stimulate higher relative anammox rates due to the preferential remineralization of N-rich compounds (*16*). Older recalcitrant OM, poor in organic N, however, will result in a smaller proportion of N loss catalyzed by anammox bacteria. Yet, integrated over both space and time, the balance between anammox and denitrification must be constrained by the flux and C/N ratio of the OM in and out of the anoxic zone.

It is also worth noting that the occurrence of nitrite accumulation in the ODZs does not significantly alter the balance between anammox and denitrification, because of the requirement that a large percentage of nitrate reduction proceeds no further than nitrite before a noticeable enrichment in fraction anammox results (fig. S3).

Furthermore, these constraints have applicability to estimating future fixed N loss. The model developed here, predicting water column denitrification rates using POM fluxes and C/N ratios, can be integrated into global biogeochemical models to provide robust constraints on present and past fixed N losses in marine suboxic regions. It is additionally helpful in evaluating the effects of ODZ expansion on future climate (*29*), potential shifts in average C/N ratios with changing atmospheric CO_2 concentrations (*30*), and negative feedbacks to global primary production via N loss.

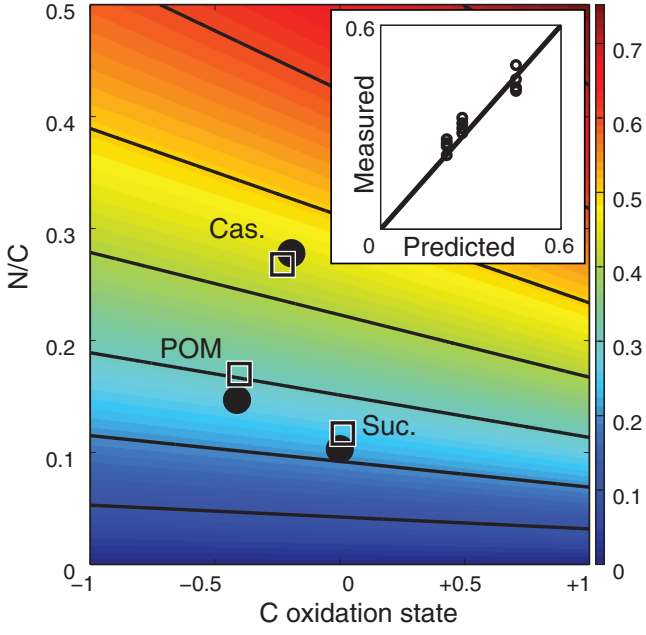

Fig. 2. Theoretical f_{amx} from OM stoichiometry. Fractions of N loss attributed to anammox (f_{amx}) are calculated by a modified version of Eq. 1 (supplementary materials text) are shown in color contours. Cas., casamino acids; Suc., sucrose. Predicted (circles) and measured (squares) f_{amx} for each OM treatment are overlaid. The inset shows these values in comparison to the expected 1:1 line.

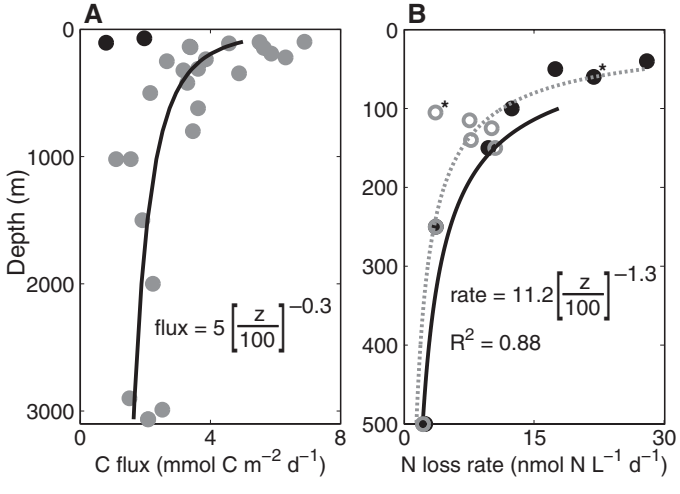

Fig. 3. Organic C-dependence of N loss. (**A**) Organic C flux previously measured (gray symbols) by benthic lander incubations (*27*) and collected in this study (black symbols) by sediment traps. The derived power law fit (black line) for the benthic lander study is included for reference. (**B**) Total N loss rates for both coastal (solid symbols) and offshore (open symbols) stations from $+^{15}NO_2^-$-only experiments. The power law best fit of these points (dashed gray line) and the theoretical rates (solid black line) driven by and derived from the organic C flux in (A) are also shown. Asterisks denote the rate experiments closest to the sediment trap deployment depths. *z*, depth; R^2, correlation coefficient.

References and Notes

1. F. A. Richards, in *Chemical Oceanography*, J. P. Riley, G. Skirrow, Eds. (Academic Press, London, 1965), vol. 1, pp. 611–643.
2. M. Bender *et al.*, *Geochim. Cosmochim. Acta* **53**, 685–697 (1989).
3. D. E. Canfield *et al.*, *Science* **330**, 1375–1378 (2010).
4. W. Koeve, P. Kähler, *Biogeosciences* **7**, 2327–2337 (2010).
5. M. Strous, J. J. Heijnen, J. G. Kuenen, M. S. M. Jetten, *Appl. Microbiol. Biotechnol.* **50**, 589–596 (1998).
6. L. A. Anderson, *Deep Sea Res. Part I Oceanogr. Res. Pap.* **42**, 1675–1680 (1995).
7. B. B. Ward *et al.*, *Nature* **461**, 78–81 (2009).
8. P. Lam *et al.*, *Proc. Natl. Acad. Sci. U.S.A.* **106**, 4752–4757 (2009).
9. T. Kalvelage *et al.*, *Nat. Geosci.* **6**, 228–234 (2013).
10. T. Dalsgaard, B. Thamdrup, L. Farías, N. P. Revsbech, *Limnol. Oceanogr.* **57**, 1331–1346 (2012).
11. A. R. Ravishankara, J. S. Daniel, R. W. Portmann, *Science* **326**, 123–125 (2009).
12. B. Kartal *et al.*, *Environ. Microbiol.* **9**, 635–642 (2007).
13. H. Ogawa, Y. Amagai, I. Koike, K. Kaiser, R. Benner, *Science* **292**, 917–920 (2001).
14. J. H. Martin, G. A. Knauer, D. M. Karl, W. W. Broenkow, *Deep Sea Res. Part A* **34**, 267–285 (1987).
15. A. H. Devol, H. E. Hartnett, *Limnol. Oceanogr.* **46**, 1684–1690 (2001).
16. B. A. Van Mooy, R. G. Keil, A. H. Devol, *Geochim. Cosmochim. Acta* **66**, 457–465 (2002).
17. F. Lipschultz *et al.*, *Deep-Sea Res. A Oceanogr. Res. Pap.* **37**, 1513–1541 (1990).
18. W. M. Berelson, *Oceanography (Wash. D.C.)* **14**, 59–67 (2001).
19. W. G. Zumft, *Microbiol. Mol. Biol. Rev.* **61**, 533–616 (1997).
20. L. A. Codispoti, T. Yoshinari, A. H. Devol, in *Respiration in Aquatic Ecosystems*, P. A. DelGiorgio, P. J. le B. Williams, Eds. (Oxford Univ. Press, New York, 2005), pp. 225–247.
21. M. M. Jensen, M. M. M. Kuypers, G. Lavik, B. Thamdrup, *Limnol. Oceanogr.* **53**, 23–36 (2008).
22. A. Paulmier, D. Ruiz-Pino, *Prog. Oceanogr.* **80**, 113–128 (2009).
23. T. Kalvelage *et al.*, *PLOS ONE* **6**, e29299 (2011).
24. D. Bianchi, J. P. Dunne, J. L. Sarmiento, E. D. Galbraith, *Global Biogeochem. Cycles* **26**, 10.1029/2011GB004209 (2012).
25. M. Strous, E. Van Gerven, J. G. Kuenen, M. Jetten, *Appl. Environ. Microbiol.* **63**, 2446–2448 (1997).
26. T. Dalsgaard, *et al.*, paper presented at the Association for the Sciences of Limnology and Oceanography Aquatic Sciences Meeting, New Orleans, 21 February 2013.
27. H. E. Hartnett, A. H. Devol, *Geochim. Cosmochim. Acta* **67**, 247–264 (2003).
28. A. Körtzinger, W. Koeve, P. Kähler, L. Mintrop, *Deep Sea Res. Part I Oceanogr. Res. Pap.* **48**, 661–688 (2001).
29. L. Stramma, G. C. Johnson, J. Sprintall, V. Mohrholz, *Science* **320**, 655–658 (2008).
30. U. Riebesell *et al.*, *Nature* **450**, 545–548 (2007).

Acknowledgments: We thank the captain and crew of the R/V *Thomas G. Thompson* for assistance in sampling; C. Buchwald and A. Morello for nutrient measurements; and B. X. Chang, D. Bianchi, and D. M. Sigman for useful discussions of this work. F. M. M. Morel provided invaluable advice in honing and improving this paper. The data presented in this paper are available in the supplementary materials. This study was supported by an NSF grant to A.H.D. and B.B.W. and a National Defense Science and Engineering Graduate Fellowship to A.R.B. A.R.B., A.H.D., and B.B.W. designed and conducted the experiments; R.G.K. collected and analyzed sediment trap material; and A.R.B. and B.B.W. wrote the manuscript with input from all authors.

Supplementary Materials

www.sciencemag.org/content/344/6182/406/suppl/DC1
Materials and Methods
f_{amx} Derivation
Figs. S1 to S3
Tables S1 and S2
References (*31*–*34*)

11 November 2013; accepted 26 March 2014
Published online 10 April 2014;
10.1126/science.1248364

www.sciencemag.org/cgi/content/full/science.1248364/DC1

Supplementary Materials for

Organic Matter Stoichiometry, Flux, and Oxygen Control Nitrogen Loss in the Ocean

Andrew R. Babbin,* Richard G. Keil, Allan H. Devol, Bess B. Ward

*Corresponding author. E-mail: babbin@princeton.edu

Published 10 April 2014 on *Science* Express
DOI: 10.1126/science.1248364

This PDF file includes:

Materials and Methods

Sites and sampling

Sampling was conducted aboard the *R/V Thomas G. Thompson* in the ETNP in March – April 2012 (Fig. S1). Two sites were chosen for intense study: coastal (20.15ºN, 106.00ºW; water depth 2200 m) and offshore (16.53ºN, 107.11ºW; water depth 3600 m) Nitrite and ammonium concentrations were determined by standard photometric methods (*31*). Ammonium was always < 20 nmol L^{-1} within the oxygen deficient zone. Water for incubations was collected from Niskin bottles into 300 mL ground glass stoppered bottles and transferred into a N_2 flushed glove bag for manipulations.

Sinking particulate organic matter (POM) was collected at 70 m (coastal) and 105 m (offshore) using a NetTrap (*32*), a large diameter (~2 m), free-drifting sediment trap, based on the design of a closing plankton net, capable of collecting large amounts of sinking POM (> 50 μm in size) in relatively short time periods (24 – 48 h). Contents of the cod end were used as the POM amendment. The POM was analyzed for C/N using an EA–IRMS at the UC Davis Stable Isotope Facility (*33*, *34*).

^{15}N tracer experiments

In addition to 3 μmol L^{-1} (final concentration) ^{15}N-nitrite tracer, treatments for amendment experiments (Fig. 1, 2, Table 1) consisted of 3 μmol L^{-1} ^{14}N-ammonium, 5.7 μmol C L^{-1} (coastal) or 4.6 μmol C L^{-1} (offshore) sinking POM, 37 μmol C L^{-1} casamino acids, 29 μmol C L^{-1} sucrose plus 3 μmol L^{-1} ammonium, 3 or 8 μmol L^{-1} O_2 plus 3 μmol L^{-1} ammonium. All organic matter additions were either autoclaved (POM) or filter sterilized (sucrose and casamino acids; 0.2 μm pore size). Furthermore, the POM was homogenized by pushing the solution repeatedly through a 23-gauge needle The oxygen was added by equilibrating water from the same depth with air. 12 mL Exetainers (LabCo, UK) were filled with 8 mL of treatment-amended seawater for incubation and purged with He for 5 minutes. Air-equilibrated seawater was injected after He-purging using a gas-tight syringe. Similarly, a second set of experiments, where only $^{15}NO_2^-$ tracer (no $^{14}NH_4^+$) was added (Fig. 3B) was conducted using the same methods. Triplicate vials were poisoned with 50% (w/v) zinc chloride at 5 time points spanning 36-

48 hours after incubation at 10ºC in the dark, and $^{29}N_2$ and $^{30}N_2$ accumulation were measured on a Europa 20/20 IRMS.

Denitrification rates were calculated from the accumulation of $^{30}N_2$ and anammox by using the binomial distribution (*7*). In parallel experiments encompassing the same depths, $^{46}N_2O$ reduction rates, representing denitrification, were also measured (Fig. S2). Because these rates were not significantly different from the denitrification rates calculated from $^{15}NO_2^-$ reduction rates reported here, we conclude that dissimilatory reduction of nitrate to ammonium did not contribute significantly to the $^{30}N_2$ accumulation.

Derivation of f_{amx} equation

To derive the balance between anammox and denitrification given organic matter of a certain composition, we assume that all organic nitrogen and the nitrate used to oxidize it are converted to N_2 gas. We begin with the stoichiometries of three anaerobic metabolisms: dissimilatory nitrate reduction to nitrite (DNRN), denitrification, and anammox, using generic organic matter composition $C_aH_bO_cN_d$ for the first two heterotrophic reactions (*4*), and an empirical (and therefore slightly imbalanced) reaction of anammox (*5*).

$$C_aH_bO_cN_d + x_1HNO_3 \rightarrow aCO_2 + dNH_3 + x_1HNO_2 + y_1H_2O \quad (1)$$

$$C_aH_bO_cN_d + x_2HNO_2 \rightarrow aCO_2 + dNH_3 + \frac{x_2}{2}N_2 + y_2H_2O \quad (2)$$

$$NH_3 + 1.32HNO_2 + 0.066HCO_3^- + 0.19H^+ \rightarrow$$
$$1.02N_2 + 0.26HNO_3 + 0.066CH_2ON_{0.15} + 2.03H_2O \quad (3)$$

Where $x_1 = 2a + \frac{b}{2} - c - \frac{3d}{2}$ and $x_2 = \frac{2x_1}{3}$. Water coefficients y_i are calculated to balance H and O and are also dependent on the organic matter stoichiometry, but are unimportant for this derivation.

We first balance NH_3 by multiplying Equation 3 by *d*, or the amount of ammonium released by the remineralization of one organic matter unit. HNO_2 is balanced by splitting the amount of organic matter used in Equation 1 from Equation 2 through multiplying them by (1–*F*) and *F* respectively. The nitrite balance then results:

$(1-F)x_1 = F\,x_2 + 1.32d$ or $F = \frac{x_1 - 1.32d}{x_1 + x_2}$.

This means that the amount of N_2 lost via denitrification is $\frac{x_2}{2}\left(\frac{x_1 - 1.32d}{x_1 + x_2}\right)$, but by substituting in with $x_i = x_i(a,b,c,d)$, $N_2^{denit} = 0.4a + 0.1b - 0.2c - 0.564d$.

As $N_2^{amx} = 1.02d$, and normalizing to organic carbon content of the organic matter,

$$f_{\mathrm{amx}} = \frac{N_2^{amx}}{N_2^{amx} + N_2^{denit}} = \frac{1.02d}{0.4a + 0.1b - 0.2c + 0.456d}$$

$$= \frac{1.02\,{}^{\mathrm{N}}/_{\mathrm{C}}}{0.4 + 0.1\,{}^{\mathrm{H}}/_{\mathrm{C}} - 0.2\,{}^{\mathrm{O}}/_{\mathrm{C}} + 0.456\,{}^{\mathrm{N}}/_{\mathrm{C}}}$$

Next, by assuming oxidation states of H (+1), O (–2) and N (–3), we can calculate the oxidation state of C in the organic molecule:

$$C_{ox} = -\,{}^{\mathrm{H}}/_{\mathrm{C}} + 2\,{}^{\mathrm{O}}/_{\mathrm{C}} + 3\,{}^{\mathrm{N}}/_{\mathrm{C}}$$

This expression can lastly be substituted into the equation for f_{amx}, giving the final equation plotted in Figure 2:

$$f_{\mathrm{amx}} = \frac{1.02\,{}^{\mathrm{N}}/_{\mathrm{C}}}{0.4 - 0.1C_{ox} + 0.756\,{}^{\mathrm{N}}/_{\mathrm{C}}}$$

Fig. S1

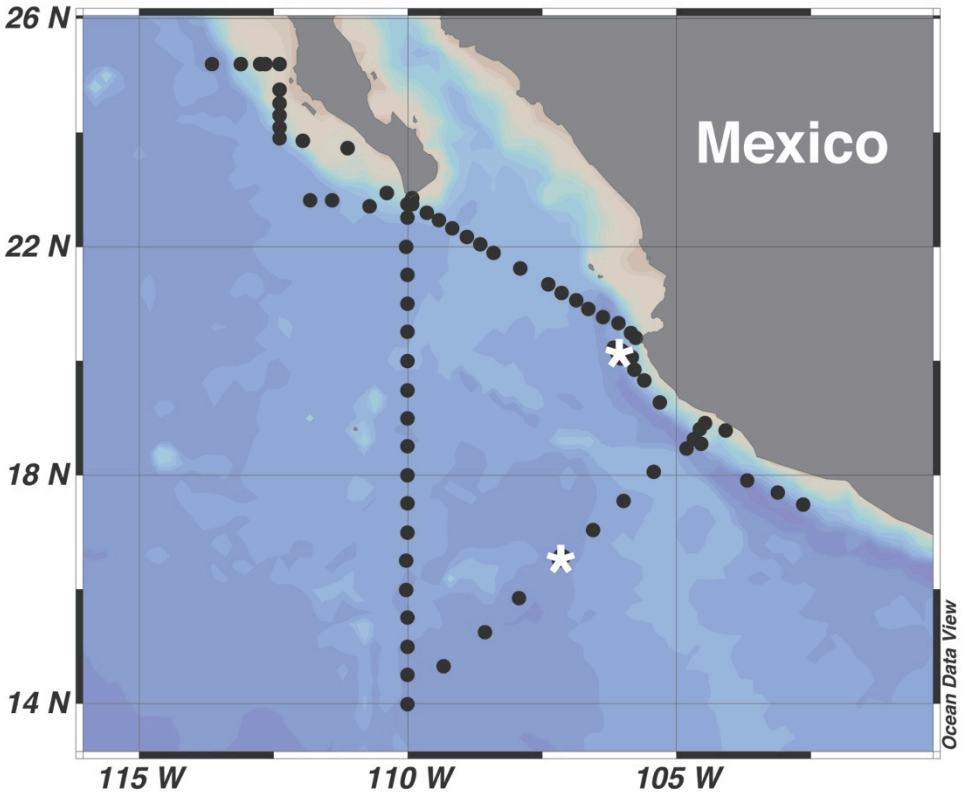

Cruise track of the *R/V Thomas G. Thompson* cruise number 278 (black circles). Asterisks denote the locations at which incubations reported here were performed.

Fig. S2

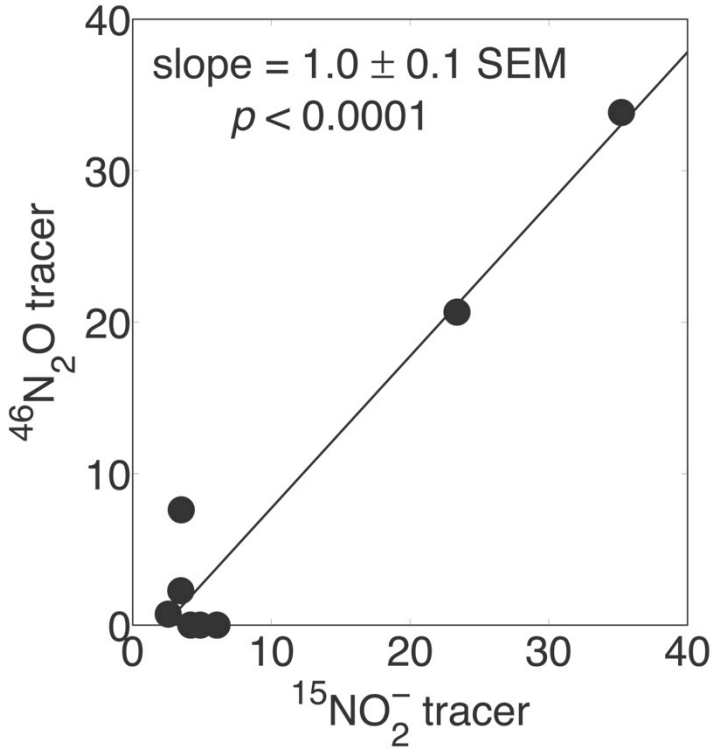

Rates of denitrification (nmol N L^{-1} d^{-1}) as measured by $^{15}NO_2^-$ and $^{46}N_2O$ tracers (no $^{14}NH_4^+$ addition) at the coastal station

Fig. S3

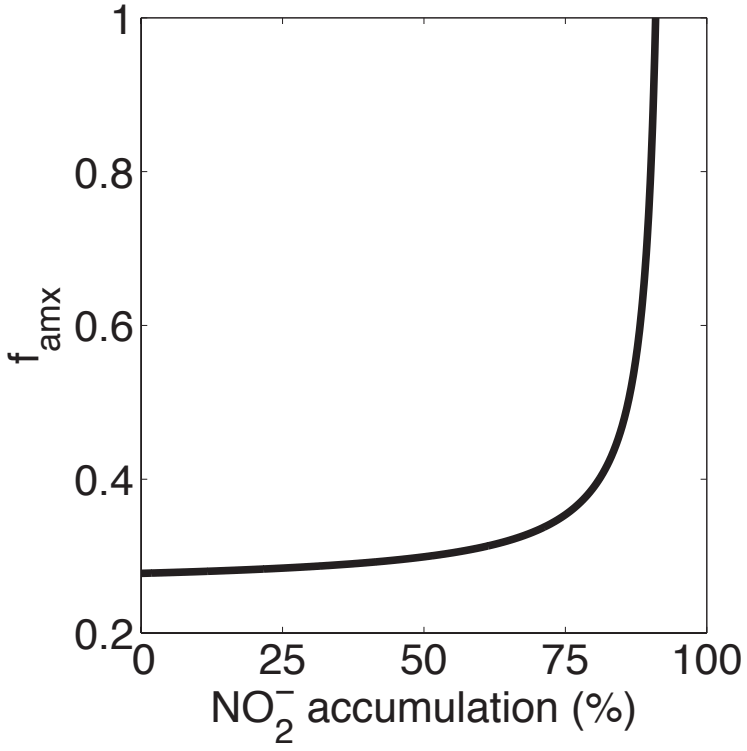

Changes to the fraction of nitrogen loss attributed to anammox given nitrite accumulation as a percentage of the net reduction from nitrate to N_2. The relationship breaks down at 91% accumulation, when there is not enough nitrite to oxidize ammonium via anammox and still have denitrification. This has been done for average marine POM stoichiometry (*6*).

Table S1.

Treatment	Coastal oxycline (60 m)	Coastal SNM (100 m)	Offshore oxycline (100 m)	Offshore SNM (150 m)
NH_4^+ only	4.7 / 3.1	2.6 / 3.3	0.8 / 0.4	2.1 / 0.9
Sucrose + NH_4^+	7.3 / 2.5	5.9 / 1.9	1.8 / 0.7	2.2 / 0.6
Casamino acids	9.3 / 7.4	9.2 / 8.6	1.6 / 1.1	3.7 / 2.7
Sinking POM	31.1 / 14.1	30.1 / 12.7	6.3 / 3.1	15.1 / 6.0
3 μmol L^{-1} O_2 + NH_4^+	0.4 / 1.1	0.1 / 0.9	0.8 / 0.4	0 / 0.9
8 μmol L^{-1} O_2 + NH_4^+	0 / 0.4	0 / 0	0 / 0	0 / 0

Measured rates of denitrification / anammox (nmol L^{-1} d^{-1}) for each treatment at both stations at the depths of the oxycline and secondary nitrite maximum (SNM).

Table S2.

Property	Coastal site	Offshore site
Depth of deployment (m)	70	105
Time of deployment (hr)	24	48
Mass collected (mg m^{-2})	88	87
Weight % organic C	27	22
Organic C sedimentation rate (mg m^{-2} d^{-1})	24	10
C/N (mol mol^{-1})	6.16	7.51

Properties of particles collected via sediment traps at the two sampling sites.

References and Notes

1. F. A. Richards, in *Chemical Oceanography*, J. P. Riley, G. Skirrow, Eds. (Academic Press, London, 1965), vol. 1, pp. 611–643.

2. M. Bender, R. Jahnke, W. Ray, W. Martin, D. T. Heggie, J. Orchardo, T. Sowers, Organic carbon oxidation and benthic nitrogen and silica dynamics in San Clemente Basin, a continental borderland site. *Geochim. Cosmochim. Acta* **53**, 685–697 (1989). doi:10.1016/0016-7037(89)90011-2

3. D. E. Canfield, F. J. Stewart, B. Thamdrup, L. De Brabandere, T. Dalsgaard, E. F. Delong, N. P. Revsbech, O. Ulloa, A cryptic sulfur cycle in oxygen-minimum-zone waters off the Chilean coast. *Science* **330**, 1375–1378 (2010). doi:10.1126/science.1196889 Medline

4. W. Koeve, P. Kahler, Heterotrophic denitrification vs. autotrophic anammox - quantifying collateral effects on the oceanic carbon cycle. *Biogeosciences* **7**, 2327–2337 (2010). doi:10.5194/bg-7-2327-2010

5. M. Strous, J. J. Heijnen, J. G. Kuenen, M. S. M. Jetten, The sequencing batch reactor as a powerful tool for the study of slowly growing anaerobic ammonium-oxidizing microorganisms. *Appl. Microbiol. Biotechnol.* **50**, 589–596 (1998). doi:10.1007/s002530051340

6. L. A. Anderson, On the hydrogen and oxygen content of marine phytoplankton. *Deep Sea Res. Part I Oceanogr. Res. Pap.* **42**, 1675–1680 (1995). doi:10.1016/0967-0637(95)00072-E

7. B. B. Ward, A. H. Devol, J. J. Rich, B. X. Chang, S. E. Bulow, H. Naik, A. Pratihary, A. Jayakumar, Denitrification as the dominant nitrogen loss process in the Arabian Sea. *Nature* **461**, 78–81 (2009). doi:10.1038/nature08276 Medline

8. P. Lam, G. Lavik, M. M. Jensen, J. van de Vossenberg, M. Schmid, D. Woebken, D. Gutiérrez, R. Amann, M. S. Jetten, M. M. Kuypers, Revising the nitrogen cycle in the Peruvian oxygen minimum zone. *Proc. Natl. Acad. Sci. U.S.A.* **106**, 4752–4757 (2009). doi:10.1073/pnas.0812444106 Medline

9. T. Kalvelage, G. Lavik, P. Lam, S. Contreras, L. Arteaga, C. R. Löscher, A. Oschlies, A. Paulmier, L. Stramma, M. M. M. Kuypers, Nitrogen cycling driven by organic matter export in the South Pacific oxygen minimum zone. *Nat. Geosci.* **6**, 228–234 (2013). doi:10.1038/ngeo1739

10. T. Dalsgaard, B. Thamdrup, L. Farías, N. Peter Revsbech, Anammox and denitrification in the oxygen minimum zone of the eastern South Pacific. *Limnol. Oceanogr.* **57**, 1331–1346 (2012). doi:10.4319/lo.2012.57.5.1331

11. A. R. Ravishankara, J. S. Daniel, R. W. Portmann, Nitrous oxide (N_2O): The dominant ozone-depleting substance emitted in the 21st century. *Science* **326**, 123–125 (2009). doi:10.1126/science.1176985 Medline

12. B. Kartal, M. M. Kuypers, G. Lavik, J. Schalk, H. J. Op den Camp, M. S. Jetten, M. Strous, Anammox bacteria disguised as denitrifiers: Nitrate reduction to dinitrogen gas via nitrite and ammonium. *Environ. Microbiol.* **9**, 635–642 (2007). doi:10.1111/j.1462-2920.2006.01183.x Medline

13. H. Ogawa, Y. Amagai, I. Koike, K. Kaiser, R. Benner, Production of refractory dissolved organic matter by bacteria. *Science* **292**, 917–920 (2001). doi:10.1126/science.1057627 Medline

14. J. Martin, G. Knauer, D. Karl, W. W. Broenkow, VERTEX: Carbon cycling in the northeast Pacific. *Deep Sea Research Part A* **34**, 267–285 (1987). doi:10.1016/0198-0149(87)90086-0

15. A. H. Devol, H. E. Hartnett, Role of the oxygen-deficient zone in transfer of organic carbon to the deep ocean. *Limnol. Oceanogr.* **46**, 1684–1690 (2001). doi:10.4319/lo.2001.46.7.1684

16. B. A. Van Mooy, R. G. Keil, A. H. Devol, Impact of suboxia on sinking particulate organic carbon: Enhanced carbon flux and preferential degradation of amino acids via denitrification. *Geochim. Cosmochim. Acta* **66**, 457–465 (2002). doi:10.1016/S0016-7037(01)00787-6

17. F. Lipschultz, S. C. Wofsy, B. B. Ward, L. A. Codispoti, G. Friedrich, J. W. Elkins, Bacterial transformations of inorganic nitrogen in the oxygen-deficient waters of the eastern tropical South Pacific Ocean. *Deep-Sea Res. A, Oceanogr. Res. Pap.* **37**, 1513–1541 (1990). doi:10.1016/0198-0149(90)90060-9

18. W. M. Berelson, The flux of particulate organic carbon into the ocean interior: A comparison of four US JGOFS regional studies. *Oceanography (Wash. D.C.)* **14**, 59–67 (2001). doi:10.5670/oceanog.2001.07

19. W. G. Zumft, Cell biology and molecular basis of denitrification. *Microbiol. Mol. Biol. Rev.* **61**, 533–616 (1997). Medline

20. L. A. Codispoti, T. Yoshinari, A. H. Devol, *Suboxic Respiration in the Oceanic Water Column*, P. A. DelGiorgio, P. J. B. Williams, Eds., *Respiration in Aquatic Ecosystems* (Oxford Univ. Press, New York, 2005), pp. 225–247.

21. M. M. Jensen, M. M. Kuypers, G. Lavik, B. Thamdrup, Rates and regulation of anaerobic ammonium oxidation and denitrification in the Black Sea. *Limnol. Oceanogr.* **53**, 23–36 (2008). doi:10.4319/lo.2008.53.1.0023

22. A. Paulmier, D. Ruiz-Pino, Oxygen minimum zones (OMZs) in the modern ocean. *Prog. Oceanogr.* **80**, 113–128 (2009). doi:10.1016/j.pocean.2008.08.001

23. T. Kalvelage, M. M. Jensen, S. Contreras, N. P. Revsbech, P. Lam, M. Günter, J. LaRoche, G. Lavik, M. M. Kuypers, Oxygen sensitivity of anammox and coupled N-cycle processes in oxygen minimum zones. *PLOS ONE* **6**, e29299 (2011). doi:10.1371/journal.pone.0029299 Medline

24. D. Bianchi, J. P. Dunne, J. L. Sarmiento, E. D. Galbraith, Data-based estimates of suboxia, denitrification, and N_2O production in the ocean and their sensitivities to dissolved O_2. *Global Biogeochem. Cycles* **26**, n/a (2012). doi:10.1029/2011GB004209

25. M. Strous, E. Van Gerven, J. G. Kuenen, M. Jetten, Effects of aerobic and microaerobic conditions on anaerobic ammonium-oxidizing (anammox) sludge. *Appl. Environ. Microbiol.* **63**, 2446–2448 (1997). Medline

26. Dalsgaard *et al*., Association for the Sciences of Limnology and Oceanography Aquatic Sciences Meeting, New Orleans, LA, 21 February 2013.

27. H. E. Hartnett, A. H. Devol, Role of a strong oxygen-deficient zone in the preservation and degradation of organic matter: A carbon budget for the continental margins of northwest Mexico and Washington State. *Geochim. Cosmochim. Acta* **67**, 247–264 (2003). doi:10.1016/S0016-7037(02)01076-1

28. A. Körtzinger, W. Koeve, P. Kähler, L. Mintrop, C:N ratios in the mixed layer during the productive season in the northeast Atlantic Ocean. *Deep Sea Res. Part I Oceanogr. Res. Pap.* **48**, 661–688 (2001). doi:10.1016/S0967-0637(00)00051-0

29. L. Stramma, G. C. Johnson, J. Sprintall, V. Mohrholz, Expanding oxygen-minimum zones in the tropical oceans. *Science* **320**, 655–658 (2008). doi:10.1126/science.1153847 Medline

30. U. Riebesell, K. G. Schulz, R. G. Bellerby, M. Botros, P. Fritsche, M. Meyerhöfer, C. Neill, G. Nondal, A. Oschlies, J. Wohlers, E. Zöllner, Enhanced biological carbon consumption in a high CO_2 ocean. *Nature* **450**, 545–548 (2007). doi:10.1038/nature06267 Medline

31. J. D. H. Strickland, T. R. Parsons, *A Practical Handbook of Seawater Analysis* (Fisheries Research Board of Canada, Ottawa, Canada, ed. 2, 1972).

32. M. L. Peterson, S. G. Wakeham, C. Lee, M. A. Askea, J. C. Miquel, Novel techniques for collection of sinking particles in the ocean and determining their settling rates. *Limnol. Oceanogr. Methods* **3**, 520–532 (2005). doi:10.4319/lom.2005.3.520

33. J. I. Hedges, J. H. Stern, Carbon and nitrogen determinations of carbonatecontaining solids. *Limnol. Oceanogr.* **29**, 657–663 (1984). doi:10.4319/lo.1984.29.3.0657

34. T. Komada, M. R. Anderson, C. L. Dorfmeier, Carbonate removal from coastal sediments for the determination of organic carbon and its isotopic signatures, $\delta^{13}C$ and $\Delta^{14}C$: Comparison of fumigation and direct acidification by hydrochloric acid. *Limnol. Oceanogr. Methods* **6**, 254–262 (2008). doi:10.4319/lom.2008.6.254

Double Helix, Doubled

Chromatin consists of genomic DNA packaged onto nucleosomes—double donut-shaped complexes of histone proteins. Roughly 150 base pairs of DNA are wrapped around each nucleosome with variable lengths of linker DNA in-between. Using cryogenic electron microscopy, **Song *et al.*** (p. 376; see the Perspective by **Travers**) determined the 11 angstrom–resolution structure of a 12-nucleosome string of DNA. The segment forms a 30-nanometer fiber structure, which is itself double-helical, like the DNA it packages.

Africa's Bane

Tsetse are blood-feeding, fast-flying flies that transmit a range of *Trypanosoma* spp. protozoan pathogens, which cause sleeping sickness in humans and their nagana in their livestock. The **International *Glossina* Genome Initiative** (p. 380) sequenced the genome of *Glossina morsitans* and identified the genes for many attributes of the tsetse's remarkable biology, including viviparity and the expression of analogs of mammalian milk proteins. Tsetse are host to several specific symbionts that appear to synthesize essential nutrients for the fly and also to hitherto undiscovered parasitoid-derived viruses. Deeper exploration of this genome will reveal what makes these fly species so host- and trypanosome specific.

Understanding N Loss

Biologically available nitrogen (N) is essential for marine plants, and shortage of N limits photosynthesis. Marine N can be removed by denitrification and anaerobic ammonia oxidation (anammox) processes, but what controls the balance between these two pathways? **Babbin *et al.*** (p. 406, published online 10 April) tested the effects of stoichiometry on N removal in the lab and found that the balance of N loss processes depends on the stoichiometry of the source organic material.

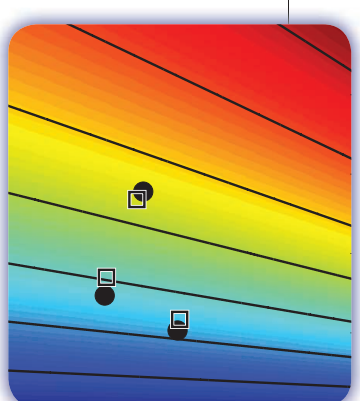

Optogenetic Insights>>

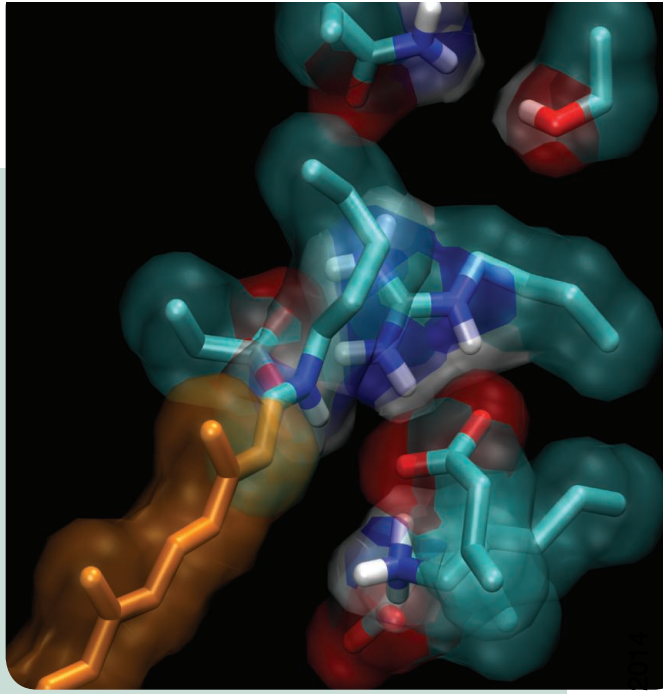

Mapping functional neural circuits for many behaviors has been almost impossible, so **Vogelstein *et al.*** (p. 386, published online 27 March; see the Perspective by **O'Leary and Marder**) developed a broadly applicable optogenetic method for neuron-behavior mapping and used it to phenotype larval *Drosophila* and thus developed a reference atlas. As optogenetic experiments become routine in certain fields of neuroscience research, creating even more specialized tools is imperative (see the Perspective by **Hayashi**). By engineering channelrhodopsin, **Wietek *et al.*** (p. 409, published online 27 March) and **Berndt *et al.*** (p. 420) created two different light-gated anion channels to block action potential generation during synaptic stimulation or depolarizing current injections. These new tools not only improve understanding of channelrhodopsins but also provide a way to silence cells.

A Dual Approach to 2 + 2

Asymmetric catalysis generally accelerates the pathway to one specific product geometry that can be manipulated by reducing the temperature to slow down competing reactions. It is more difficult to be selective in photochemical reactions, but in the [2 + 2] coupling of olefins to make four-membered rings, **Du *et al.*** (p. 392; see the Perspective by **Neier**) used a ruthenium catalyst that absorbs visible light to activate the substrates below the frequency threshold where they absorb intrinsically. Then a second—a chiral Lewis acid—catalyst directs the product stereochemistry. A major advantage of the dual reactions is that each catalyst can be tuned independently.

Wetted Apatite

The long-running story of the dry Moon was rewritten a few years ago when hydrogen-bearing glass spherules were discovered. The highest water contents are found in lunar apatite, at levels suspiciously comparable to the water content of Earth apatites. **Boyce *et al.*** (p. 400, published online 20 March; see the Perspective by **Anand**) now show that the water content of lunar apatite is not a reliable indicator of the abundance of water in mare basalts. The existence of apatite with high water content is an almost inevitable consequence of the loss of tiny amounts of fluorine-rich apatite from a melt and replacement by hydrogen and is thus no indication of a "wet" Moon.

House or Face?

The neural mechanisms of spatial attention are well known, unlike nonspatial attention. **Baldauf and Desimone** (p. 424, published online 10 April) combined several technologies to identify a fronto-temporal network in humans that mediates nonspatial object-based attention. There is a clear top-down directionality of these oscillatory interactions, establishing the inferior-frontal cortex as a key source of nonspatial attentional inputs to the inferior-temporal cortex. Surprisingly, the mechanisms for nonspatial attention are strikingly parallel to the mechanisms of spatial attention.

No Light Control

Light is the main source of energy for plants and is also used as a signal for growth and development: Indeed, it can modulate up to a fifth of the entire transcriptome in both *Arabidopsis thaliana* and rice. **Petrillo *et al.*** (p. 427, published online 10 April) show that light can affect gene expression through alternative splicing of the serine-arginine rich protein *At-RS31*, required for proper plant growth. But photoreceptors are not involved; rather, a mobile retrograde signal from the chloroplast controls the alternative splicing of *At-RS31*.

CREDITS (TOP TO BOTTOM): JONAS WIETEK AND HISROSHI WATANABE; BABBIN *ET AL.*

Additional summaries

Magnified Flare-Up

The rise and fall of the luminosity of a supernova detected in 2010 was typical for its class, but its apparent brightness was 30 times greater than similar events. **Quimby *et al.*** (p. 396) compared spectra from the time of peak brightness and after the supernova faded, from which they concluded that something was interfering with our line of sight to the supernova. A previously unknown foreground galaxy turned out to be acting as a lens, bending and magnifying the light from the supernova. Potentially, spacetime warping like this could allow direct testing of cosmic expansion.

Deep Freeze

Geologists usually consider glaciers and ice sheets to be gigantic abrasives, scouring the ground beneath them and carving out relief on the underlying landscapes. **Bierman *et al.*** (p. 402, published online 17 April) show that this is not always the case. They found that the silt at the very bottom of the Greenland Ice Sheet Project 2 core contained significant amounts of beryllium-10, an isotope produced in the atmosphere by cosmic rays and which adheres to soils when it is deposited on them. Hence, the dust at the bottom of the ice sheet indicates the persistence of a landscape under 3000 meters of glacial ice that is millions of years old.

RNA Heteroplasmy

Like nuclear DNA, the mitochondrial genome has to be posttranscriptionally modified to function properly; however, among individuals, mitochondrial RNA (mtRNA) transcripts vary in ways that are poorly understood. **Hodgkinson *et al.*** (p. 413) looked at mtRNA editing events and post-transcriptional methylation in more than 700 individuals. Interestingly, variation at the ninth position within transfer RNAs showed a high frequency of variation that, in some cases, is genetically attributable.

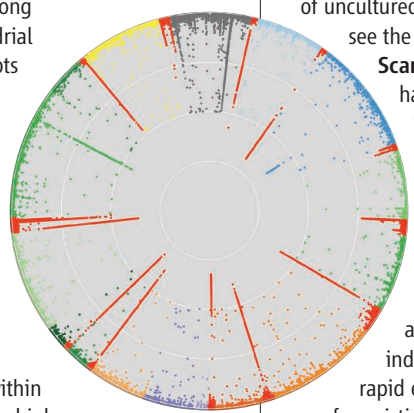

CREDIT: HODGKINSON *ET AL.*

Oceans of Cyanobacterial Diversity

What does it mean to be a global species? The marine cyanobacterium *Prochlorococcus* is ubiquitous and, arguably, the most abundant and productive of all living organisms. Although to our eyes the seas look uniform, to a bacterium the ocean's bulk is a plethora of microhabitats, and by large-scale single-cell genomic analysis of uncultured cells, **Kashtan *et al.*** (p. 416; see the Perspective by **Bowler and Scanlan**) reveal that *Prochlorococcus* has diversified to match. This "species" constitutes a mass of subpopulations—each with million-year ancestry—that vary seasonally in abundance. The subpopulations in turn have clades nested within that show covariation between sets of core alleles and variable gene content, indicating flexibility of responses to rapid environmental changes. Large sets of coexisting populations could be a general feature of other free-living bacterial species living in highly mixed habitats.

Published by AAAS